An ^{17}O NMR Investigation of Crystalline Sodium Metasilicate: Implications for the Determination of Local Structure in Alkali Silicates

T. M. Clark and P. J. Grandinetti*

Department of Chemistry, The Ohio State University, 120 West 18th Avenue, Columbus, Ohio 43210-1173

P. Florian

CNRS-CRMHT, 1D Av. de la Recherche Scientifique, 45071 Orléans Cedex 2, France

J. F. Stebbins

Department of Geological and Environmental Sciences, Stanford University, Stanford, California 94305

Received: April 9, 2001; In Final Form: September 4, 2001

Crystalline sodium metasilicate, Na_2SiO_3, has been investigated by ^{29}Si, ^{23}Na, and ^{17}O MAS NMR spectroscopy. The ^{17}O quadrupolar coupling parameters have been measured for the bridging oxygen (BO) and nonbridging oxygen (NBO) sites. Ab initio calculations have also been performed for clusters modeling these oxygen sites, as well as other sites in crystalline silicates of known structure. On the bases of ab initio calculations, parametrized equations are discussed which describe trends in the BO ^{17}O quadrupolar coupling parameters. The agreement between these parametrized equations and reported values for a variety of crystalline environments is shown to be quite good. The ab initio calculated NBO ^{17}O quadrupolar coupling parameters are also in agreement with measured results for Na_2SiO_3 and analogous crystalline alkali silicates such as α-$Na_2Si_2O_5$ and $Li_2Si_2O_5$.

1. Introduction

A multinuclear NMR investigation can provide a comprehensive description of local structure around a variety of atoms in a material, even in the absence of long range order. Advances in solid-state NMR[1−3] during the past decade have greatly improved this approach, placing quadrupolar nuclei such as ^{17}O, ^{23}Na, and ^{11}B nearly on par with more commonly studied spin $^1/_2$ nuclei such as ^1H, ^{13}C, ^{29}Si, and ^{31}P. The remaining task, however, is to bring our understanding of the relationships between the NMR parameters of quadrupolar nuclei and local structure to the same level that currently exists for spin $^1/_2$ nuclei.

Because of the historical difficulties associated with doing ^{17}O solid-state NMR, relatively little is known of the relationships between ^{17}O NMR parameters and structure when compared to the more commonly used spin $^1/_2$ probes. Investigations by Tossell and co-workers[4−6] were one of the earliest to have shown that ab initio quantum mechanical calculations can be a powerful tool for researchers trying to connect measured ^{17}O NMR parameters to structural features. Indeed, the ab initio trends predicted in ^{17}O quadrupolar coupling parameters with Si−O−Si bond angle by Tossell and co-workers have been experimentally verified using ^{17}O DAS,[7] and these theoretically derived trends have been indispensable in quantifying structural distributions in silicate glasses.[8]

A crucial step in confirming theoretically derived trends between NMR parameters and structure is to compare experimental results obtained for crystalline compounds with those predicted by calculations. At present, the agreement between experimental and theoretical results for relatively simple oxygen environments, such as bridging oxygen sites in SiO_2 polymorphs, has been quite good.[9] Although ab initio calculations have been performed for more complex oxygen environments which include modifier cations,[10] it is important to determine how well these calculated trends are in agreement with experimental results.

The experimentally determined ^{17}O quadrupolar coupling parameters of Na_2SiO_3, reported here, allow us to consider oxygen sites which are more structurally complex. For example, the bridging oxygen site in Na_2SiO_3 is coordinated by two sodium cations, each at a distance of 2.40 Å, and two silicon atoms, both at a distances of 1.62 Å, considerably longer than Si−O distances found in SiO_2 polymorphs such as quartz, cristobalite, or coesite. The nonbridging oxygen site is also remarkable because it is, to our knowledge, a rare example of a nonbridging oxygen site in an alkali silicate for which a known crystal structure exists and a reliable measurement of the ^{17}O NMR chemical shift, quadrupolar coupling constant, and asymmetry parameter may be readily obtained since the bridging oxygen and nonbridging oxygen resonances are well resolved. In previous studies[11] severe overlap of bridging and nonbridging resonances in combination with the inherent low sensitivity of ^{17}O solid-state NMR made the determination of NMR parameters, particularly the quadrupolar coupling asymmetry parameter somewhat suspicious.

Thus, Na_2SiO_3 is ideally suited for an investigation which continues the process of joining experimentally determined ^{17}O quadrupolar coupling parameters, ab initio calculations, and a discussion of local structure at oxygen sites. In the present multinuclear NMR investigation, ^{29}Si and ^{23}Na results also serve to confirm the identity of the sample. The ^{17}O results for the bridging and nonbridging oxygen sites in Na_2SiO_3 are then

* Corresponding author. FAX: 614-292-1685. E-mail: grandinetti.1@osu.edu.

10.1021/jp011289p CCC: $20.00
Published on Web 11/13/2001

TABLE 1: Experimental NMR Parameters in $NaSiO_3$ Obtained from Lineshape Analyses[a]

		chemical shift parameters			quadrupole coupling parameters	
nucleus	site	δ_{iso}^{cs}, ppm	Δ^{cs}, ppm	η_{cs}	C_q, MHz	η_q
^{23}Na		22.1 ± 0.5			1.40 ± 0.1	0.7 ± 0.1
^{29}Si		-76.7 ± 0.2	-76 ± 10	0.7 ± 0.3		
^{17}O	BO	63 ± 2			4.20 ± 0.2	0.58 ± 0.05
	NBO	39 ± 2			2.43 ± 0.1	0.17 ± 0.05

[a] The simulations of the experimental spectra were performed using a modified version of the Bruker WinFit software package.[12] Simulation conditions included second-order quadrupolar broadened line shapes under infinite spinning speed conditions. Gaussian distributions in C_q with a standard deviation of $\sigma = 0.19$ and 0.09 MHz were used for simulating the NBO ^{17}O and ^{23}Na resonances, respectively. A Herzfeld−Berger analysis[13] of the spinning sidebands for the ^{29}Si spectrum was performed to obtained the chemical shift anisotropy (CSA) parameters.

discussed in relation to previous experimental results on other crystalline alkali silicates, such as α-$Na_2Si_2O_5$ and $Li_2Si_2O_5$. Ab initio calculations for the bridging and nonbridging oxygen sites are also considered and compared with results from crystalline alkali silicates.

2. Experimental Methods

2.1. Sample Synthesis. Approximately 40% ^{17}O-enriched SiO_2 powder was prepared by the hydrolysis of $SiCl_4$ with $H_2{}^{17}O$. Crystalline $Na_2SiO_3$was prepared by initially decarbonating a mixture of ^{17}O-enriched SiO_2 with a stoichiometric quantity of Na_2CO_3 and 0.1% cobalt oxide (to decrease T_1) at 1033 K for 15 h. The sample was then melted at 1473 K and crystallized by slow cooling to 1053 K. The sample was then reground and recrystallized at the same temperature for 15 h. All heating took place under Ar gas. Due to the hygroscopic nature of the product, care was taken to avoid exposing the sample to the atmosphere and an Ar-gas substituted glovebox was utilized during the handling of the sample, i.e., the rotor packing for the nuclear magnetic resonance (NMR) measurements. This synthesis procedure results in single phase polycrystalline Na_2SiO_3, as confirmed by X-ray diffraction, and the identity and purity of the crystalline sample used in this investigation has been confirmed by magic angle spinning (MAS) NMR spectroscopic results.

2.2. NMR Spectroscopy. ^{23}Na, ^{29}Si, and ^{17}O magic angle spinning NMR experiments experiments were performed at 9.4 T on a Chemagnetics CMX II spectrometer using a home-built probe. Experiments were done at ambient temperature with sample spinning rates between 12 and 14 kHz, unless otherwise noted. Samples were contained in a silicon nitride rotor with a 4 mm diameter. Recycle times were obtained using a saturation recovery experiment. Chemical shift data references are 1M NaCl for ^{23}Na, TMS for ^{29}Si and tap water for ^{17}O. The ^{23}Na spectrum was acquired using a Bloch decay sequence with a flip angle below $\pi/8$ (pulse length of 0.5 microseconds), a recycle delay of 1.0 s, and a spectral width of 50 kHz. The ^{29}Si spectrum was also acquired using a Bloch decay sequence with a nonselective pulse length of 0.54 microseconds, a recycle delay of 15.0 s, and a spectral width of 25 kHz. An echo sequence ($90-\tau-180-$acquire) was used to collect the ^{17}O spectra with a $\pi/2$ and π pulse lengths of 7.0 and 14.0 microseconds, respectively, an echo shift of 9.0 milliseconds, a recycle delay of 660 s, and a spectral width of 20 kHz. The experimental NMR spin coupling parameters obtained from line shape analyses of these three spectra are given in Table 1.

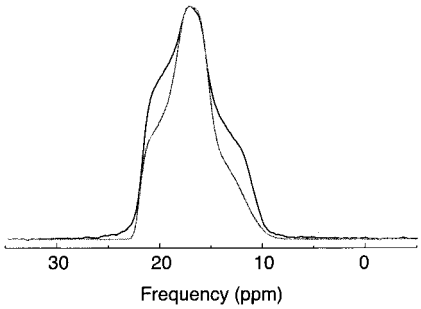

Figure 1. Experimental ^{23}Na MAS NMR spectrum (upper line) of crystalline Na_2SiO_3 shown along with numerical simulation. Details of the numerical simulation are given in the caption of Table 1.

3. Theoretical Methods

Ab initio calculations were performed using GAUSSIAN 94[14] at a restricted Hartree−Fock level with a 6-31+G(d) basis set used for all atoms. GAUSSIAN 94 calculates the traceless electric field gradient (efg) tensor and outputs its Cartesian tensor elements. These calculated efg tensor elements are related to the quadrupolar coupling constant C_q and quadrupolar coupling asymmetry parameter η_q according to

$$C_q = e^2Q\langle q_{zz}\rangle/h, \quad \text{and} \quad \eta_q = \langle q_{xx}\rangle - \langle q_{yy}\rangle/\langle q_{zz}\rangle \quad (1)$$

where $e\langle q_{xx}\rangle$, $e\langle q_{yy}\rangle$, and $e\langle q_{zz}\rangle$ are the principal components of the electric field gradient tensor defined such that $|\langle q_{zz}\rangle| > |\langle q_{yy}\rangle| > |\langle q_{xx}\rangle|$ and Q is the nuclear electric quadrupole moment. For ^{17}O, a value of $e^2Q/h = -6.11$ MHz a.u.^{3} was used to convert the q_{zz} output from Gaussian into the ^{17}O quadrupolar coupling constant.

As noted by Xue and Kanzaki,[15] the nuclear quadrupole moment cannot be directly measured and is typically derived from the experimental C_q value and the calculated EFG for the free atom. The eQ value is therefore dependent on the manner in which the EFG is calculated, i.e., the basis set(s) and method employed, and it has been common in many ab initio studies to treat the eQ value as an adjustable parameter when calculating the quadrupolar coupling constant.[9,15,16] In this work we have chosen to calibrate the absolute C_q values obtained by ab initio methods with several experimental results, an approach consistent with a previous investigation.[10]

Model clusters were constructed to represent the oxygen environments in Na_2SiO_3 and other silicates. The clusters used to model bridging oxygen environments are similar to those described previously[10] with hydrogen atoms being added to terminate dangling oxygen bonds. A variety of clusters were employed for the study of nonbridging oxygen sites. The justification for the construction of these model clusters is addressed below.

4. Experimental Results and Discussion

4.1. Sodium-23. The ^{23}Na MAS NMR spectrum obtained in the present investigation is shown in Figure 1. On the bases of diffraction studies,[17] we expect one sodium site in Na_2SiO_3, coordinated by five oxygen atoms with Na−O distances ranging from 2.2 to 2.5 Å. This site has a geometry of a distorted trigonal bipyramidal and four of the oxygen coordinated to the sodium are nonbridging oxygen with the fifth being a bridging oxygen. Fitting the ^{23}Na spectrum to a single site, however, gives a somewhat unsatisfactory result and suggests a sodium site which is at least partially disordered. A spectrum similar in appearance was reported by Xue and Stebbins[18] and the line shape attributed

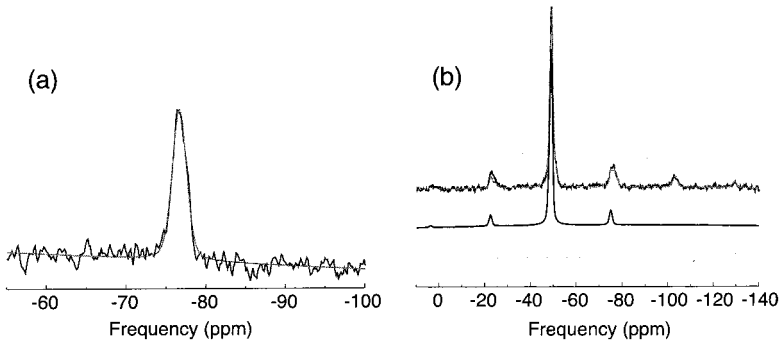

Figure 2. ^{29}Si MAS NMR spectrum collected for crystalline Na_2SiO_3 at high and low spinning speeds, approximately 12 and 2.1 kHz, respectively. In (a) a narrow region of the spectrum at high spinning speed is shown which includes the resonance from the silicon site in Na_2SiO_3. The spectrum (b), at low speed, includes signal from the silicon nitride rotor and the sample. In each plot the experimental data is shown along with a simulation fitting the data. Components of the simulation are shown below the spectrum.

to partial disordering of sodium or to multiple crystallographically unique sodium sites. Subsequent work, however, has indicated that Na_2SiO_3 is prone to breaking into needle-shaped fragments when crushed[19] and so the line shape distortion may be partly attributed to preferred crystalline orientations due to anisotropic particle shapes in the crushed sample. In either case, the derived parameters are in good approximation and agree with reported values.[18]

Previous investigations have correlated the ^{23}Na isotropic chemical shift, δ_{iso}^{Na}, with the structural features of sodium sites in alkali silicates[18,20,21] and mixed-alkali silicates.[22] Ab initio methods, employed to compliment these findings,[23] have noted that δ_{iso}^{Na} in these systems is primarily dependent on the Na−O distance, the coordination number of the sodium, and the bonding character of the oxygen. An empirical relationship between δ_{iso}^{Na} and the Na−O distance in crystalline silicate compounds has been reported[18,24] and indicates that δ_{iso}^{Na} increases in an approximately linear manner with decreasing d_{Na-O}. This is consistent with the relatively large δ_{iso} value reported here since the Na−O distances for Na_2SiO_3 are rather small (in comparison with other sodium silicates), having an average d_{Na-O} value of only 2.38 Å. In addition, as discussed in an ab initio study,[23] δ_{iso}^{Na} increases with increasing sodium coordination numbers when the Na−O distance is constant. Structurally, however, an increase in coordination number is typically accompanied by an increase in d_{Na-O}; thus, these two influences on δ_{iso}^{Na} are competing. The result of this competition is that the largest δ_{iso}^{Na} values occur for sodium coordination numbers near four or five,[23] a finding in agreement with that observed for the sodium in Na_2SiO_3 with 5-fold coordination. The nature of the oxygen coordinated to the sodium is also an important factor. The δ_{iso}^{Na} value is somewhat larger when sodium is coordinated by nonbridging oxygen versus bridging oxygen.[18] Therefore, the degree of depolymerization of the silicate network plays a role in determining the sodium chemical shift. Increasing depolymerization of the network leads to sodium primarily coordinated by nonbridging oxygen and thus having larger δ_{iso}^{Na} values. This influence may be exemplified by comparing the δ_{iso}^{Na} values of 22.1 ppm for Na_2SiO_3 versus 16.9 ppm for α-$Na_2Si_2O_5$.[18] In both cases the coordination number of the sodium is five and the average d_{Na-O} values are approximately equal. The silicate network, however, differ with Na_2SiO_3 and α-$Na_2Si_2O_5$ containing $Q^{(2)}$ and $Q^{(3)}$ tetrahedra, respectively.

The quadrupolar coupling parameters of $C_q = 1.46$ MHz and $\eta_q = 0.71$ have been previously reported for the sodium site in Na_2SiO_3.[20] From the spectrum in Figure 1 we obtain a quadrupole coupling constant of $C_q = 1.40 \pm 0.1$ MHz and an asymmetry parameter of $\eta_q = 0.7 \pm 0.1$. Although the agreement between these reported values are good, the apparent disorder evident from the ^{23}Na spectrum precludes a more precise determination of the parameters. Qualitatively, the quadrupolar coupling constant and asymmetry parameter are expected to be near zero for regular tetrahedra or octahedral coordinations, and nonzero for trigonal bipyramidal or quadratic pyramidal symmetries, with the largest C_q values present for planar geometries.[20] Thus, the observed ^{23}Na C_q and η_q values are qualitatively consistent with this prediction. In general, however, correlations between structure and quadrupolar coupling parameters for sodium in silicates may be ambiguous since the contribution of even the most asymmetric first coordination sphere structures around sodium to the ^{23}Na electric field gradient can be comparable to contributions from higher coordination sphere structures, making it difficult to more precisely predict the local structure of sodium sites based solely on the quadrupolar coupling parameters.

4.2. Silicon-29. The only silicon site in Na_2SiO_3 is a tetrahedrally coordinated $Q^{(2)}$ site. A high spinning speed (12 kHz) spectrum showing only the region containing the resonance from the silicon site in Na_2SiO_3 is shown in Figure 2a. The full spectrum collected at a low spinning speed of 2.1 kHz is shown in Figure 2b and includes an additional peak at approximately −50 ppm attributed to the silicon nitride rotor. The ^{29}Si isotropic chemical shift, chemical shift tensor axiality, and chemical shift tensor asymmetry parameters of $\delta_{iso}^{Si} = -76.7$ ppm, $\Delta^{Si} = -76 \pm 10$ ppm, and $\eta_{cs}^{Si} = 0.7 \pm 0.3$, respectively, were measured for the Na_2SiO_3 sample from the high speed spectrum and by fitting of the sidebands present in the low spinning speed spectrum. The previously reported chemical shift parameters for Na_2SiO_3, i.e., $\delta_{iso}^{Si} = -77.6$ ppm, $\Delta^{Si} = -78$ ppm, and $\eta_{cs}^{Si} = 0.52 \pm 0.3$,[25] are in good agreement with the values reported here.

In general, silicon tetrahedrally coordinated by oxygen have δ_{iso}^{Si} values in the range of −60 to −120 ppm, and those in a $Q^{(2)}$ environment within the range of −74 to −95 ppm.[25] The axiality and the asymmetry parameters, which are defined elsewhere,[26] are sensitive to the Q-species of the silicon atoms. For example, both $Q^{(0)}$ and $Q^{(4)}$ species have low Δ^{Si} values due to their highly symmetric environments. It is also possible to distinguish $Q^{(2)}$ species, which have large η values, from $Q^{(1)}$ or $Q^{(3)}$ environments which have η values near zero. A Δ^{Si} value between −50 and −90 ppm and the large η value reported for the silicon site in Na_2SiO_3 is typical of $Q^{(2)}$ sites in alkali silicates.[27] As expected, all three ^{29}Si chemical shift parameters in Na_2SiO_3 are in good agreement with those of other $Q^{(2)}$ environments.

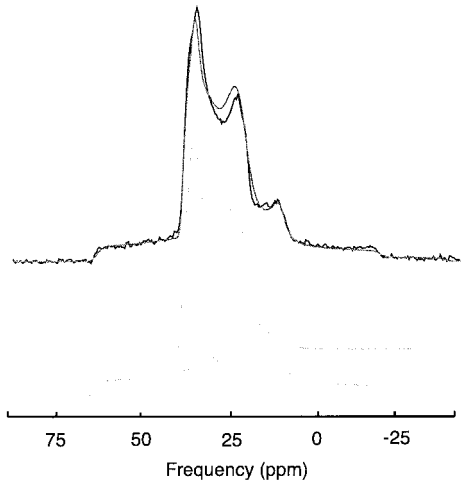

Figure 3. ^{17}O MAS NMR spectrum for Na_2SiO_3. The experimental data is shown along with a simulation fitting the data. Components of the simulation are shown below the spectrum. Details of the numerical simulation are given in the caption of Table 1.

4.3. Oxygen-17. There are two oxygen sites in Na_2SiO_3, a bridging oxygen site and a nonbridging oxygen site, present in the BO/NBO ratio of 33/67. The bridging oxygen links two SiO_4 tetrahedra and is also coordinated by two sodium cations that are each 2.4 Å from the bridging oxygen. The nonbridging oxygen is coordinated by four sodium cations and these cations, together with the silicon, form a distorted trigonal bipyramidal structure. The Si−NBO distance is 1.592 Å, a value typical of Si atoms in a $Q^{(2)}$ environment.

The ^{17}O MAS NMR spectrum is presented in Figure 3 and the chemical shift and quadrupolar coupling parameters derived from the line shape simulation for the bridging and nonbridging oxygen sites are given in Table 1. The spectrum is characterized by a broad, lower intensity resonance with a C_q value of 4.20 MHz and a δ_{iso}^{cs} value of 63 ppm, and a narrow higher intensity resonance with a C_q value of 2.43 MHz and a δ_{iso}^{cs} value of 39 ppm. The ratio of integrated intensities of the two line shapes is approximately 40/60 and are assigned to the bridging and nonbridging oxygen sites, respectively. This assignment is also consistent with the respective quadrupolar coupling constants and chemical shifts for the two resonances.[2,7,8,25,28−31] While a good fit to the bridging oxygen line shape was obtained assuming a single site, a less than satisfactory fit to a single site was obtained for the nonbridging oxygen line shape. An improved fit to the nonbridging oxygen line shape, shown in Figure 3, was obtained using a Gaussian distribution in C_q values centered about 2.43 MHz with a standard deviation of 0.15 MHz. This implies that there may be partial disordering of sodium primarily about the nonbridging oxygen, and would also be consistent with the disorder implied by the ^{23}Na spectrum.

In general, the quadrupolar coupling constant of the nonbridging oxygen is expected to be approximately half of that for the bridging oxygen in silicates. This factor of 2 difference follows from a simple point charge model of the electric field gradient where the nonbridging oxygen is coordinated by one silicon instead of two. Much more subtle structural details around each of these sites, however, can be determined from the quadrupolar coupling parameters, and this will be discussed in the next section.

As with the ^{29}Si chemical shift, it is expected that the paramagnetic contribution to the ^{17}O chemical shift will be more sensitive to structural changes around oxygen than the diamagnetic contribution.[35] Thus it is not surprising that, just like ^{29}Si, strong linear correlations exist between ^{17}O chemical shift and bond distances in the first coordination sphere. This trend is strongly pronounced for oxygen coordinated by alkaline earth cations in the series BeO, MgO, CaO, SrO, and BaO, or for the group IIB oxides in the series ZnO, CdO, HgO.[36] Timken et al.[32] first observed this trend in a series of alkaline earth metasilicates for both bridging and nonbridging oxygen, although the effect was more pronounced for the nonbridging oxygen. A similar trend appears for oxygen coordinated by alkali cations, although the effect is less pronounced, as demonstrated by Maekawa et al.[11] in a series of crystalline and glassy alkali disilicates. This trend in alkali silicates is most apparent in the ^{17}O DAS results for a series of mixed alkali (sodium or potassium) disilicate glasses by Vermillion et al.[29] These results, which are summarized in Figure 4 for bridging and nonbridging oxygen sites modified by alkali and alkaline earth cations, clearly demonstrate the strong correlation between the ^{17}O chemical shift and structural features in the first coordination sphere.

In contrast to ^{17}O quadrupolar coupling parameters, the use of ^{17}O isotropic chemical shifts as a probe of more subtle structural features has been elusive as it is becoming apparent that structural variations out to third coordination sphere can

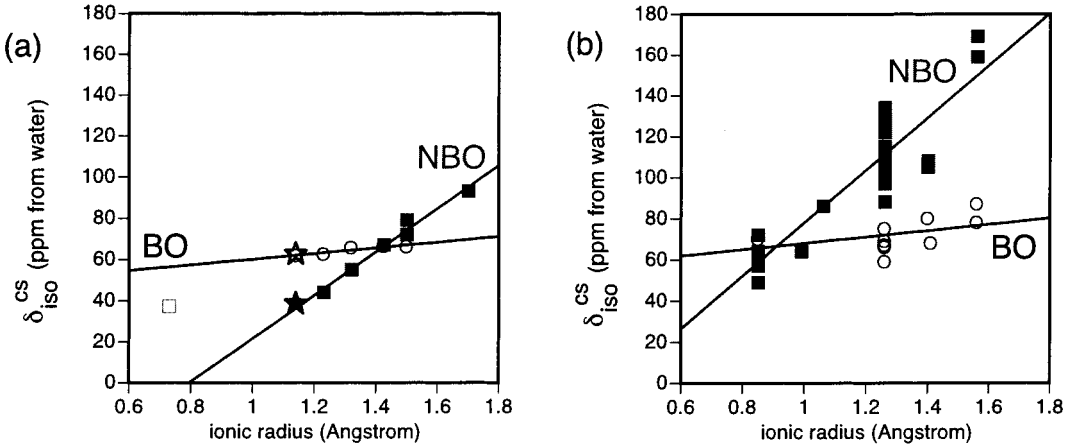

Figure 4. Plot of ^{17}O chemical shift versus average metal-ion radius in (a) alkali and (b) alkaline earth silicates. Bridging and nonbridging oxygen are shown as open and filled symbols, respectively, in both plots. The Na_2SiO_3 results from this investigation are represented as a star. Results for $(Na_xK_{1-x})_2Si_2O_5$ glasses[29] and crystalline alkali disilicates[11] and for crystalline[30,32] and glassy[33] alkaline earth silicates are shown as squares. The nonbridging oxygen site in $Li_2Si_2O_5$ (an outlier) is shown as an open square. Best fit lines for the BO and NBO are $y = 13.6x + 46.4$ ($r^2 = 0.972$) and $y = 105x - 83.5$ ($r^2 = 0.985$), respectively, for the alkali silicates, and $y = 15.2x + 52.8$ ($r^2 = 0.905$) and $y = 128x - 50.4$ ($r^2 = 0.875$), respectively, for the alkaline earth silicates. Effective ionic radii data are from ref 34.

TABLE 2: ^{17}O Experimental and ab Initio Calculated Results for the Bridging Oxygen Sites in Crystalline Silica Polymorphs and Alkali Silicates[a]

	bridging oxygen environment					experimental NMR parameters				ab initio predicted		
compound	∠Si−O−Si	d(Si−O), Å	no. of coord. modifiers	d(M−O), Å	ref	δ_{cs}, ppm	C_q/MHz	η	ref	C_q	η	ratio
α-quartz	143.6°	1.60, 1.61	none	n/a	38	39 ± 2	5.25 ± 0.1	0.18 ± 0.02	39	−5.81	0.202	0.90
cristobalite	146.47°	1.60, 1.60	none	n/a	40	40 ± 2	5.3 ± 0.1	0.125 ± 0.005	41	−5.82	0.144	0.91 ± 0.02
coesite	180.00°	1.59, 1.59	none	n/a	42	29 ± 1	6.05 ± 0.05	0.000 ± 0.005	7	−6.31	0.020	0.96 ± 0.01
	142.56°	1.61, 1.61	none	n/a	42	41 ± 1	5.43 ± 0.05	0.166 ± 0.005	7	−5.78	0.215	0.94 ± 0.01
	149.53°	1.61, 1.60	none	n/a	42	53 ± 1	5.52 ± 0.05	0.169 ± 0.005	7	−6.04	0.144	0.91 ± 0.01
	144.46°	1.61, 1.61	none	n/a	42	57 ± 1	5.45 ± 0.05	0.168 ± 0.005	7	−5.95	0.208	0.91 ± 0.01
	137.22°	1.62, 1.62	none	n/a	42	58 ± 1	5.16 ± 0.05	0.292 ± 0.005	7	−5.74	0.30	0.90 ± 0.01
$Li_2Si_2O_5$	156°	1.60, 1.60	none	n/a	43	108 ± 10	5.6 ± 0.3	0.55 ± 0.2	11	−6.43	0.05	0.87 ± 0.05
	128°	1.64, 1.65	1 Li	2.04	43	35 ± 10	4.05 ± 0.3	0.05 ± 0.1	11	−4.94	0.74	0.82 ± 0.06
Na_2SiO_3	133.7°	1.67, 1.68	2 Na	2.40, 2.40	17	63 ± 2	4.20 ± 0.2	0.58 ± 0.05	this work	−5.2	0.49	0.82 ± 0.04
α-$Na_2Si_2O_5$	160.04°	1.61, 1.61	none	n/a	44	52 ± 10	5.74 ± 0.2	0.2 ± 0.1	11	−6.46	0.05	0.89 ± 0.03
	138.93°	1.64, 1.64	1 Na	2.39	44	74 ± 10	4.67 ± 0.2	0.3 ± 0.1	11	−5.64	0.37	0.83 ± 0.04
$K_2Si_4O_9$	134.7°	1.64, 1.66	2 K	2.98, 2.98	45	62.5 ± 1	4.45 ± 0.05	0.35 ± 0.05	31	−5.56	0.41	0.80 ± 0.01
	141.7°	1.59, 1.78	2 K	2.79, 3.00	45	97 ± 1	4.90 ± 0.05	0.20 ± 0.05	31	−5.00	0.22	0.98 ± 0.01

[a] Model clusters used in the ab initio calculations are denoted in column 6, and the ratio value in last column refers to C_q (experimental)/C_q (calculated).

also have a significant influence on the chemical shift. For example, in coesite[7] the experimentally measured ^{17}O isotropic chemical shifts for the bridging oxygen appear to be entirely uncorrelated to Si−O−Si angle and Si−O distance. Xue and Kanzaki[9] performed ab initio calculations employing clusters expanded out to four coordination spheres to model each of the silicate bridging oxygen linkages in coesite and found that while the ^{17}O C_q and η_q values converged within the first coordination sphere of each oxygen, it was necessary to extend the cluster calculations out to higher coordination spheres to obtain qualitative agreement with the ^{17}O isotropic chemical shifts. In work by Bull et al.[37] four complete coordination spheres around each oxygen site were needed in an ab initio calculations to obtain reasonable agreement with experimentally observed ^{17}O chemical shifts in siliceous zeolite faujasite. As a result of this strong dependence of ^{17}O chemical shifts on structural variations beyond the first coordination sphere, we have limited our theoretical investigations in the next section to the ^{17}O quadrupolar coupling parameters. Further theoretical work on ^{17}O chemical shifts is currently in progress.

5. Theoretical Results and Discussion

We employed ab initio calculations on model clusters depicting the bridging oxygen and the nonbridging oxygen sites and compared these to ^{17}O quadrupolar coupling parameters measured in crystalline compounds of known structure. Thus, in addition to Na_2SiO_3 results presented here, we have used the specific oxygen geometries found in the crystalline compounds α-quartz, cristobalite, coesite, α-$Na_2Si_2O_5$, $Li_2Si_2O_5$, and $K_2Si_4O_9$, whose crystal structures are known and the NMR parameters for the oxygen sites have been experimentally determined.[11]

5.1. Bridging Oxygen. Clusters modeling the bridging oxygen sites were constructed by placing atoms in their crystallographic lattice positions and capping dangling oxygen with hydrogen atoms. These clusters were used, after geometry optimization of hydrogen positions only, in ab initio calculations to obtain the bridging oxygen C_q and η_q parameters. Selected structural parameters for the bridging oxygen sites are given in Table 2.

As expected, the calculated C_q values need to be scaled to bring them into agreement with the experiments. All scalings, shown in Table 2, fall into a narrow range centered around 0.89, indicating that the clusters used in these calculations are reasonable models for the different oxygen sites. With a few notable exceptions there is generally good agreement between the experimental and ab initio predicted quadrupolar coupling parameters for each site. There is good agreement between calculated η_q values and experiment for all the crystalline silica polymorphs, and again with a few notable exceptions, there is also good agreement between calculated and experimental η_q values for all alkali silicates. The exceptions occur in cases where severe overlap of bridging and nonbridging resonances in combination with the inherent low sensitivity of ^{17}O solid-state NMR made the experimental determination of η_q problematic.

5.1.1. General Trends. In general, there are a number of structural features that play a role in determining the ^{17}O quadrupolar coupling parameters of the bridging oxygen, with the most significant features occurring in the first coordination sphere of the bridging oxygen. The relevant features are the nature of the two coordinating network forming cations,[32,46,47] the T−O−T′ linkage angle,[4−6] the T−O bond distances,[48] and the nature and number of coordinating network modifier cations.[10] For the quadrupolar coupling parameters contributions from beyond the first coordination sphere of the bridging oxygen appear to be secondary in importance. For example, Xue and Kanzaki[9] performed ab initio calculations employing clusters expanded out to four coordination spheres to model each of the silicate bridging oxygen linkages in coesite and obtained a slightly improved agreement with the experimental trends, with corrections on the order of a few percent in the ^{17}O C_q and η_q values.

Taking these first coordination sphere structural features into account, we employ the following general expression for the ^{17}O quadrupolar coupling parameters of a bridging oxygen in an alkali silicate:

$$C_q(\Omega,n_M) = a\left(\frac{1}{2} + \frac{\cos\Omega}{\cos\Omega - 1}\right)^{\alpha} + n_M \Delta C_q^M \qquad (2)$$

$$\eta_q(\Omega,n_M) = b\left(\frac{1}{2} - \frac{\cos\Omega}{\cos\Omega - 1}\right)^{\beta} + \Delta\eta_q^M(n_M) \qquad (3)$$

Here Ω is the Si−O−Si angle, n_M is the number of coordinating alkali metal cations, and ΔC_q^M and $\Delta\eta_q^M$ are the shifts in C_q and

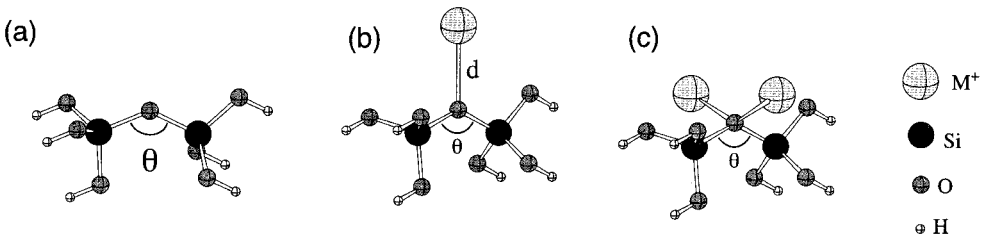

Figure 5. Molecular geometries used to investigate the effect of Si−O−Si bond angle variation and the presence of alkali cations near the bridging oxygen atom on its ^{17}O quadrupolar coupling parameters. (a) Staggered configuration without modifier cations present,(b) staggered configuration with one modifier in the plane of the Si−O−Si angle and in the plane that bisects the Si−O−Si angle, (c) staggered configuration with two modifier cations in the plane that bisects the Si−O−Si angle and each at an angle 45° away from the plane of the Si−O−Si angle.

TABLE 3: Best Fit Parameters for Equations 2 and 3, and the Linear Fit to the C_q and η_q ab Initio Data (C_q Scaled by 0.88) for Clusters with Zero, One, or Two Coordinating Alkali Cations

	C_q dependence			η_q dependence			C_q, η_q correlation	
cation(s)	a, MHz	α	ΔC_q^M, MHz	b	β	$\Delta\eta_q^M$	slope, MHz	intercept, MHz
none	−5.85	1.78	0.00	5.03	1.09	0.000	2.28	−5.82
1 Li^+ (d_{LiO} = 2.0 Å)	−5.85	1.70	−0.66	6.58	1.18	0.364	2.17	−5.95
2 Li^+ (d_{LiO} = 2.0 Å)	−5.85	1.71	−0.68	7.46	1.23	0.116	1.90	−4.65
1 Na^+ (d_{NaO} = 2.5 Å)	−5.85	1.69	−0.43	6.13	1.18	0.235	2.11	−5.86
2 Na^+ (d_{NaO} = 2.5 Å)	−5.85	1.71	−0.43	6.03	1.18	0.061	2.13	−5.07
1 K^+ (d_{KO} = 2.8 Å)	−5.85	1.70	−0.21	5.76	1.17	0.131	2.15	−5.79
2 K^+ (d_{KO} = 2.8 Å)	−5.85	1.72	−0.24	5.55	1.15	0.000	2.29	−5.33

η_q due to the presence of these alkali cations coordinated at their equilibrium distances. The parameters a, α, b, and β are additional adjustable parameters that have been calibrated using both experiment and ab initio calculations. Of course, these expressions are by no means unique in their ability to describe these relationships, and other expressions have been used previously.[6,8,49] On the bases of these relationships, a plot of C_q versus η_q is also expected to be nearly linear for bridging oxygen clusters, with the C_q-intercept decreasing in magnitude with increasing modifier field strength and coordination.

As discussed by Clark and Grandinetti[48] the quadrupolar coupling constant is also linearly dependent on the Si−O distance. This dependence, however, is not explicitly indicated in equations 2 and 3, but rather is included implicitly by assuming that the Si−O distance is energetically constrained by the Si−O−Si angle as described by Newton and Gibbs.[50] Thus its effect is included in the adjustable parameters of the two expressions. This implies, however, that the ^{17}O quadrupolar coupling constant of bridging oxygen linking highly "strained" tetrahedra with Si−O distances deviating from the local energy minimum associated with a given bridging oxygen angle may not be well described by these equations. In such cases, the quadrupolar asymmetry parameter would serve as a better probe of the Si−O−Si angle.

These relationships were calibrated by performing ab initio calculations for the model clusters $(OH)_3Si-O-Si(OH)_3$, $M[(OH)_3Si-O-Si(OH)_3]^+$, and $M_2[(OH)_3Si-O-Si(OH)_3]^{2+}$, where M = Na, Li, or K. A graphical representation of these various clusters are shown in Figure 5. Although previous results were obtained for clusters containing Li- and Na-cations[10] we have extended these calculations to include the effects of coordination by K-cations. In each case, the Si−O−Si angle was varied between 120° and 180°. Modifying cations were placed at a distance typically observed in crystalline alkali silicates, i.e., 2.0 Å for the Li-cluster, 2.5 Å for the Na-cluster, and 2.8 Å for the K-cluster. The best fit of the ab initio data to eqs 2 and 3 yields the parameters in Table 3, and the associated best fit curves are shown as solid lines in Figure 6. Experimental and calculated results are also included for bridging oxygen sites in alkali silicate compounds. For comparison, results are also provided for silicate samples which do not have modifiers present, i.e., coesite[7] and cristobalite.[31]

With the exception of the O2 site in $K_2Si_4O_9$ (which is structurally unique, joining tetrahedrally and octahedrally coordinated Si-atoms), there is excellent agreement between the experimental C_q values and the predicted general trends. As shown in Figure 6, the experimental values are in agreement with the predicted trend in C_q, i.e., the experimental points are near the solid line which incorporates the best fit parameters listed in Table 3. For a variety of bridging oxygen sites the C_q parameter is systematically reduced in magnitude when modifying alkali cations are present, with this decrease being related to the cation's field-strength.

Given that the general trends, which calculated using highly symmetric model clusters (shown in Figure 5), still apply to the wide range of structures found in crystalline compounds suggests that the C_q parameter is primarily dependent on the Si−O−Si angle, and the type and number of modifier cations present. Within the range of geometries characteristic of crystalline alkali silicates, other structural features, such as cation orientation, appear to have a relatively minor influence on C_q.[10] Thus these results confirm that the C_q parameter can serve as a reliable probe of the Si−O−Si angle and the number of coordinating modifiers for the bridging oxygen in alkali silicates over a wide range of geometries.

In general, the experimental results for the asymmetry parameter follow the general trends with the magnitude of η_q increasing for a given Si−O−Si bond angle when alkali modifiers are present. There are, however, a few notable exceptions. Both of the η_q values for bridging oxygen sites in $Li_2Si_2O_5$ are far from the expected values; the experimental value for the bridging oxygen site with a single Li modifier is much too low (Figure 6b) and the second site, which does not include a modifying cation, has an experimental value much too high (Figure 6b). The experimental results for these particular sites also diverge significantly from the predicted trends when plotting η_q versus C_q (Figure 6b). Not surprisingly, the ab initio calculated η_q values for bridging oxygen in clusters

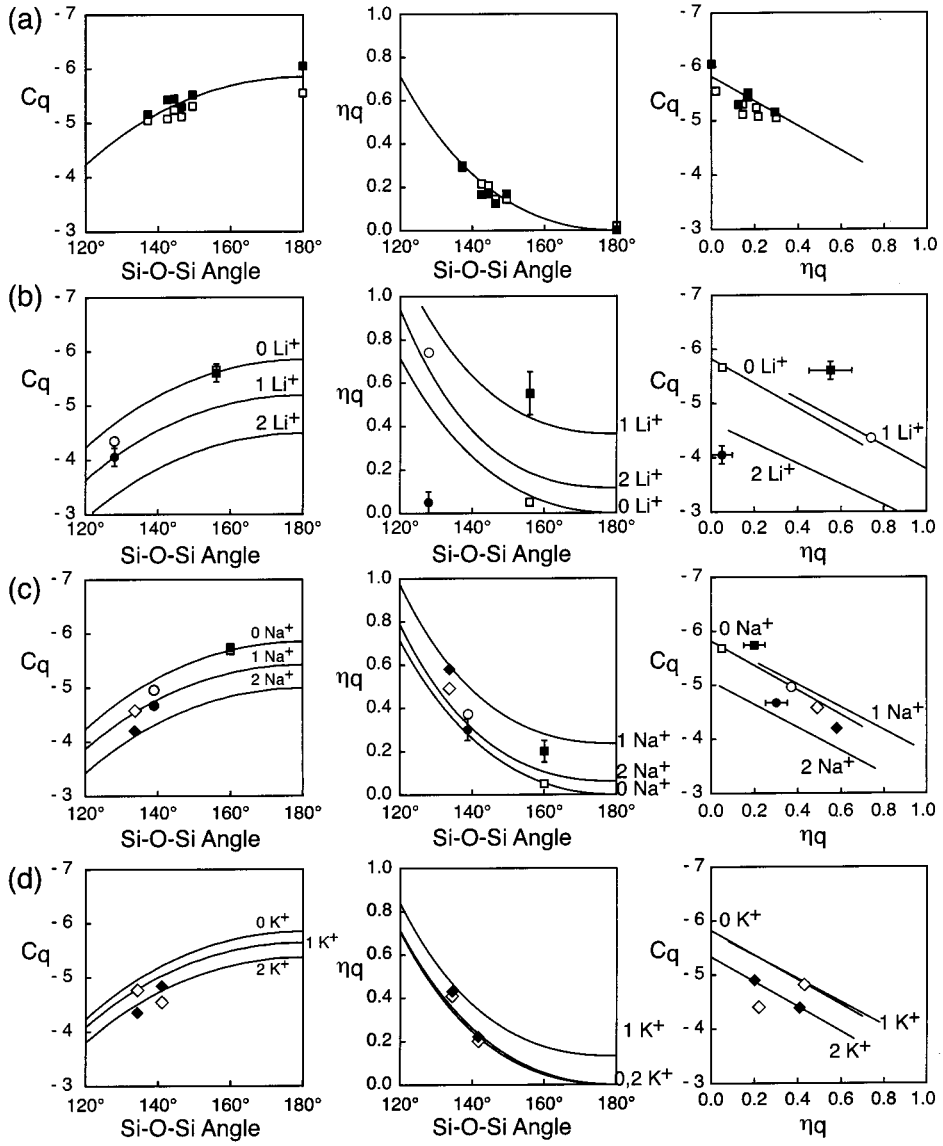

Figure 6. Comparison of general trends (solid lines), experimental (filled symbols), and calculated ab initio results (open symbols: C_q scaled by 0.88). Experimental and ab initio predicted quadrupolar coupling parameters for specific bridging oxygen sites coordinated to no alkali cations are represented as squares, to one alkali cation as circles, and to two alkali cations as diamonds. In (a) are plots of quadrupolar coupling parameters of the silica polymorphs, in (b) are plots for the lithium silicate $Li_2Si_2O_5$, in (c) sodium silicates $NaSiO_3$, α-$Na_2Si_2O_5$, and (d) potassium silicate O2 site in $K_2Si_4O_9$.

designed to match the exact geometries of the bridging oxygen in each crystal structure are in excellent agreement with the general trends in every example considered, including the sites whose experimental η_q values are in poor agreement with the general trends. This supports our argument that the experimental values for the outliers may be suspect. In general it is more difficult to extract precise η_q values than C_q values, suggesting that while the C_q parameters for these sites may be correct, many η_q values may require reconsideration. Indeed, inspection of the published experimental MAS spectrum for the $Li_2Si_2O_5$ sample[11] reveals that the bridging oxygen site resonances are broadened, overlapping, and display marginal signal/noise, and thus are difficult to completely resolve. By combining recent advances such as RAPT[51] with dynamic-angle spinning[2,52] or FASTER[53] with multiple-quantum magic-angle spinning[3] these compounds should be revisited for a more accurate η_q measurement.

5.2. Nonbridging Oxygen. A limited number of ^{17}O experimental results are found in the literature for nonbridging oxygen sites in silicates, borosilicates, and aluminosilicates.[11,29−33,54,55] If one considers only nonbridging oxygen sites in alkali silicates, the number of experimental results becomes even smaller.[11,29,31] For this reason it is more difficult to establish trends between structure and NMR parameters in the same manner as was done for bridging oxygen sites, although a few general trends are apparent. As discussed above, the chemical shift values for nonbridging oxygen atoms in silicates are sensitive to the type of metal cation modifying the network. Also, the C_q value for nonbridging oxygen sites is approximately one-half the magnitude (near 2.3 MHz) of that for bridging oxygen sites.

The NMR parameters are given in Table 4 for the nonbridging oxygen site in Na_2SiO_3. Parameters are also given for nonbridging oxygen sites in α-$Na_2Si_2O_5$ and $Li_2Si_2O_5$. The experimentally determined C_q values for these sites range from 2.4 to 2.45(±0.1) MHz and η_q values range from 0.1 to 0.2. These C_q values are similar to reported values for NBO in crystalline or glassy alkali silicates.[11,29,31] A salient characteristic for NBO sites, exemplified here and in the literature, is their narrow range of C_q values. The η_q values are also similar to each other, being nonzero and within the reported standard error. This similarity in quadrupole coupling parameters for Na_2SiO_3, α-$Na_2Si_2O_5$,

TABLE 4: ^{17}O Experimental and ab Initio Calculated Results for the Nonbridging Oxygen Sites in Alkali Silicates[a]

	experimental NMR parameters			ab initio predicted			
compound	δ_{iso}^{cs} (ppm)	C_q (MHz)	η	model cluster	C_q	η	ratio
Na_2SiO_3	39 ± 2	2.43 ± 0.1	0.17 ± 0.05	$[(OH)_3Si-O-Na_4]^{+3}$	−3.00	0.42	0.80
				$[(OH)_3Si-O-(Na\text{-}O\text{-}H)_4]^{-1}$	−3.35	0.17	0.72
				$[(OH)_3Si-O-(Na\text{-}O\text{-}H)_4(H_2O)_7)]^{-1}$	−3.50	0.11	0.70
α-$Na_2Si_2O_5$	36 ± 2	2.40 ± 0.1	0.20 ± 0.1	$[(OH)_3Si-O-(Na\text{-}O\text{-}H)_4]^{-1}$	−3.09	0.17	0.77
$Li_2Si_2O_5$	38 ± 2	2.45 ± 0.01	0.10 ± 0.1	$[(OH)_3Si-O-(Li\text{-}O\text{-}H)_4]^{-1}$	−3.24	0.17	0.76

[a] Experimental results for α-$Na_2Si_2O_5$ and $Li_2Si_2O_5$ are from ref 11. Model clusters used in the ab initio calculations are denoted in column 5, and the ratio value in the last column refers to C_q (experimental)/C_q (calculated).

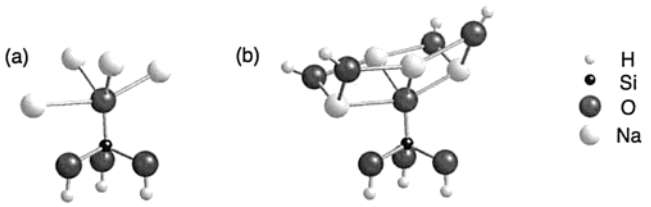

Figure 7. Model clusters depicting the non-bridging oxygen site in Na_2SiO_3: (a) Model cluster $[(OH)_3Si-O-Na_4]^{+3}$ and (b) model cluster $[(OH)_3Si-O-(Na-O-H)_4]^{-1}$.

and $Li_2Si_2O_5$ is not unexpected since the NBO sites in these structures are comparable, i.e., they each have four modifier cations.

In crystalline alkali silicates, nonbridging oxygen atoms are typically coordinated to three, four, or five modifier cations.[33] The resulting geometry of cations about the nonbridging oxygen is commonly trigonal bipyramidal or octahedral. In rare instances, a distorted trigonal bipyramidal structure is observed such that only three modifier cations are closely coordinated to the nonbridging oxygen. These geometries are the result of several constraints, including the need of the cations to compensate the charge of the anion and also steric factors. To understand the qualitative differences in quadrupolar coupling parameters when NBO are coordinated by three, four, or five alkali cations, we can assume that the *z* component for the NBO efg principal axis system lies along the Si−O bond and treat the coordinating alkali cations as classical point charges. In such a simple point charge calculation one finds that the C_q value is largest for an octahedral geometry with five Na modifiers, decreases for a tetrahedral geometry with three Na modifiers, and is smallest for clusters with four modifiers. Differences in the asymmetry parameter are also present, with η being near zero for all of these geometries except the trigonal bipyramidal structure with four modifiers. Deviations from these regular coordination geometries and differences in the charges of the cations will affect both quadrupolar coupling parameters.

To explore these effects in a more quantitative fashion one needs to adopt a more rigorous theoretical approach. For example, using periodic Hartree−Fock ab initio theoretical methods Winkler et al.[56] calculated the electric field gradient tensors for the three nonbridging oxygen sites in crystalline forsterite, Mg_2SiO_4, and obtained excellent agreement with experiment.[54] As an alternative, we have taken the approach employed for the bridging oxygen in the previous section, namely, the nonbridging oxygen environment in Na_2SiO_3 was modeled by examining the clusters shown in Figure 7. Using the cluster $[(OH)_3Si-O-Na_4]^{+3}$ (Figure 7a) we examined the effect of the first coordination sphere of the nonbridging oxygen on its electric field gradient. The cluster $[(OH)_3Si-O-(Na-O-H)_4]^{-1}$ (Figure 7b) is larger and includes oxygen in the second coordination sphere which are approximately 3.5 Å from the nonbridging oxygen and also interstitial to the sodium. The calculated quadrupolar coupling parameters are shown in Table 4. Hydrogen atoms were also added to this structure to terminate dangling oxygen bonds and bring the charge of the cluster close to neutral. In a similar manner, clusters representing the nonbridging oxygen sites in α-$Na_2Si_2O_5$ and $Li_2Si_2O_5$ were constructed. For each of these clusters four alkali cations are located near the nonbridging oxygen and these cations, along with the silicon, form a distorted trigonal bipyramidal geometry.

The calculated C_q values for the nonbridging oxygen clusters expanded to include oxygen atoms coordinated to the modifying cations are in reasonable agreement, after scaling, with the experimental data. All scalings, shown in Table 4, fall into a narrow range, again indicating that the clusters used in these calculations are reasonable models for the different oxygen sites.

When examining the calculated η_q values for the Na_2SiO_3-clusters it becomes apparent that the ab initio results are dependent on the cluster used to model the nonbridging oxygen site. For the cluster $[(OH)_3Si-O-Na_4]^{+3}$ a nonzero η_q value of 0.42 is obtained, in agreement with the point charge model, but much larger than the experimentally determined value of 0.17. With an increase of cluster size to $[(OH)_3Si-O-(Na-O-H)_4]^{-1}$, η_q decreases to a value of 0.17 and is in closer agreement with the experimental result. Calculations for even larger model clusters, such as $[(OH)_3Si-O-(Na-O-H)_4\text{-}(H_2O)_7)]^{-1}$, also produced results within the standard error of the experimental data and significantly increased the computational cost. These findings were also noted for the disilicate clusters, with calculated η_q values being difficult to reconcile with experimental results for the clusters which do not include oxygen atoms coordinated to the modifying cations.

It is not surprising that ab initio calculated η_q values for clusters which are extended to include the second nearest neighbors about the nonbridging oxygen are in better agreement with the experimental results than those which ignore the larger coordination sphere. The need for larger clusters around nonbridging compared to bridging oxygen is reasonable since the first coordination sphere's contribution to the nonbridging oxygen efg is approximately half that of the bridging oxygen. That is, higher coordination sphere structures have a greater perturbative effect on the nonbridging oxygen efg than on the bridging oxygen efg. Thus a larger cluster is required to properly model the nonbridging oxygen efg. This is also a likely explanation for the need to use slightly different scaling factors to obtain agreement with experimental C_q values for the nonbridging oxygen compared to the bridging oxygen sites. In general, the clusters used to model the nonbridging oxygen sites in this investigation are comparable in size to those employed in other investigations.[23] Although additional experimental data for alkali silicates are required to more fully understand the influence of modifying cations on ^{17}O quadrupolar coupling parameters, it is clear that that quadrupolar coupling parameters are calculable for both bridging and nonbridging oxygen sites if the model cluster is of sufficient size.

Conclusions

Using ^{23}Na, ^{29}Si, and ^{17}O NMR the local environments of sodium, silicon and oxygen sites have been probed and the results discussed in relation to the reported crystal structure. By joining experimental and ab initio calculated results, we have described the relationship between structure and NMR parameters for bridging oxygen sites in alkali silicates. As suggested in an earlier investigation[10], the magnitude of the ^{17}O quadrupolar coupling constant and asymmetry parameter for bridging oxygen sites in alkali silicates is primarily influenced by the Si−O−Si bond angle. Alkali cations systematically shift the C_q value for a given Si−O−Si bond angle lower in magnitude. This shift increases in magnitude as the field strength of the cation increases, or when the number of modifying increases from one to two. For a given Si−O−Si bond angle, η_q is increased in magnitude by the presence of modifier cations. This increase is more pronounced when a single modifier cation (rather than two cations) is coordinated to the bridging oxygen. Parametrized equations for C_q and η_q, calibrated using ab initio calculations on simple model clusters, have been confirmed by examining a variety of bridging oxygen environments in crystalline alkali silicates, including Na_2SiO_3, α-$Na_2Si_2O_5$, and $Li_2Si_2O_5$. We have also demonstrated that clusters, expanded out to the second coordination sphere of a nonbridging oxygen, can also serve as effective models in ab initio calculations of ^{17}O quadrupolar coupling parameters for nonbridging oxygen in solids.

Acknowledgment. This work was supported by a grant from the National Science Foundation (Grant CHE-9807498).

References and Notes

(1) Llor, A.; Virlet, J. *Chem. Phys. Lett.* **1988**, *152*, 248−253.
(2) Chmelka, B. F.; Mueller, K. T.; Pines, A.; Stebbins, J.; Wu, Y.; Zwanziger, J. W. *Nature* **1989**, *339*, 42−43.
(3) Frydman, L.; Harwood: J. S. *J. Am. Chem. Soc.* **1995**, *117*, 5367−5369.
(4) Tossell, J. A.; Lazzeretti, P. *Chem. Phys. Lett.* **1987**, *112*, 205.
(5) Tossell, J. A.; Lazzeretti, P. ¢¢*Phys. Chem. Miner.* **1988**, *15*, 564.
(6) Lindsay, C. G.; Tossell, J. A. *Phys. Chem. Miner.* **1991**, *18*, 191.
(7) Grandinetti, P. J.; Baltisberger, J. H.; Werner, U.; Pines, A.; Farnan, I.; Stebbins, J. F. *J. Phys. Chem.* **1995**, *99*, 12341−12348.
(8) Farnan, I.; Grandinetti, P. J.; Baltisberger, J. H.; Stebbins, J. F.; Werner, U.; Eastman, M. A.; Pines, A. *Nature* **1992**, *358*, 31−35.
(9) Xue, X.; Kanzaki, M. *Solid State NMR* **2000**, *16*, 245−259.
(10) Vermillion, K. E.; Florian, P.; Grandinetti, P. J. *J. Chem. Phys.* **1998**, *108* (17), 7274−7285.
(11) Maekawa, H.; Florian, P.; Massiot, D.; Kiyono, H.; Nakamura, M. *J. Phys. Chem.* **1996**, *100* (17), 5525−5532.
(12) Massiot, D.; Thiele, H.; Germanus, A. *Bruker Report* **1994**, *140*, 43−46.
(13) Herzfeld, J.; Berger, A. E. *J. Chem. Phys.* **1980**, *73*, 6021.
(14) Frisch, M. J.; Trucks, G. W.; Schlegel, H. B.; Gill, P. M. W.; Johnson, B. G.; Robb, M. A.; Cheeseman, J. R.; Keith, T.; Petersson, G. A.; Montgomery, J. A.; Raghavachari, K.; Al-Laham, M. A.; Zakrzewski, V. G.; Ortiz, J. V.; Foresman, J. B.; Peng, C. Y.; Ayala, P. Y.; Chen, W.; Wong, M. W.; Andres, J. L.; Replogle, E. S.; Comperts, R.; Martin, R. L.; Fox, D. J.; Binkley, J. S.; Defrees, D. J.; Baker, J.; Stewart, J. P.; Head-Gordon, M.; Gonzalez, C.; Pople, J. A. Gaussian 94, revision b.3; Gaussian, Inc.: Pittsburgh, PA, 1995.
(15) Xue, X.; Kanzaki, M. *Phys. Chem. Miner.* **1998**, *26*, 14−30.
(16) Xue, X.; Kanzaki, M. *J. Phys. Chem. B* **1999**, *103*, 10816−10830.
(17) McDonald, W. S.; Cruickshank, D. J. *Acta Crystallogr.* **1967**, *22*, 37−43.
(18) Xue, X.; Stebbins, J. F. *Phys. Chem. Miner.* **1993**, *20*, 297−307.
(19) George, A. M.; Richet, P.; Stebbins, J. F. *Am. Mineral.* **1998**, *83*, 1277−1284.
(20) Koller, H.; Engelhardt, G.; Kentgens, A. P.; Sauer, J. *J. Phys. Chem.* **1994**, *98*, 1544−1551.
(21) Angeli, F.; Delaye, J. M.; Charpentier, T.; Petit, J. C.; Ghaleb, D.; Faucon, P. *J. Non-Cryst. Solids* **2000**, *276*, 132−144.
(22) Stebbins, J. F. *Solid State Ionics* **1998**, *112*, 137−141.
(23) Tossell, J. A.*Phys. Chem. Miner.* **1999**, *27*, 70−80.
(24) Maekawa, H.; Nakao, T.; Shimokawa, S.; Yokokawa, T. *Phys. Chem. Miner.* **1997**, *24*, 53.
(25) Stebbins, J. F. Nuclear Magnetic Resonance Spectroscopy of Silicates and Oxides in Geochemistry and Geophysics. In *Handbook of Physcial Constants*; Ahrens, T. H., Ed.; American Geophysical Union: Washington, DC, 1994.
(26) Zhang, P.; Dunlap, C.; Florian, P.; Grandinetti, P. J.; Farnan, I.; Stebbins, J. F. *J. Non-Cryst. Solids* **1996**, *204*, 294−300.
(27) Emerson, J. F.; Stallworth, P. E.; Bray, P. J. *J. Non-Cryst. Solids* **1989**, *113*, 253.
(28) Mueller, K. T.; Wu, Y.; Chmelka, B. F.; Stebbins, J.; Pines, A. *J. Am. Chem. Soc.* **1991**, *113*, 32.
(29) Florian, P.; Vermillion, K. E.; Grandinetti, P. J.; Farnan, I.; Stebbins, J. F. *J. Am. Chem. Soc.* **1996**, *118*, 3493−3497.
(30) Mueller, K. T.; Baltisberger, J. H.; Wooten, E. W.; Pines, A. *J. Phys. Chem.* **1992**, *96*, 7001.
(31) Xue, X.; Stebbins, J. F.; Kanzaki, M. *Am. Miner.* **1994**, *79*, 31.
(32) Timken, H. K. C.; Schramm, S. E.; Kirkpatrick, R. J.; Oldfield, E. *J. Phys. Chem.* **1987**, *91*, 1054−1058.
(33) Stebbins, J. F.; Oglesby, J. V.; Xu, Z. *Am. Mineral.* **1997**, *82*, 1116−1124.
(34) Huheey, J. E. *Inorganic Chemistry*, 3rd ed.; Harper & Row: New York, 1983.
(35) Engelhardt, G.; Michel, D. *High-Resolution Solid-State NMR of Silicates and Zeolites*; John Wiley & Sons: Chichester, 1987.
(36) Turner, G. L.; Chung, S. E.; Oldfield, E. *J. Magn. Reson.* **1985**, *64*, 316−324.
(37) Bull, L. M.; Cheetham, A. K.; Anupold, T.; Reinhold: A.; Samoson, A.; Sauer, J.; Bussemer, B.; Lee, Y.; Gann, S.; Shore, J.; Pines, A.; Dupree, R.; *J. Am. Chem. Soc.* **1998**, *120*, 3510−3511.
(38) Kihara, K. *Eur. J. Mineral.* **1990**, *2* (1), 63−77.
(39) Dupree, R. Nuclear Magnetic Resonance as a Structural Probe of SiO_2. In *Structure and Imperfections in Amorphous and Crystalline SiO_2*; Devine, R., Durand, J. P., Dooryhee, E., Eds.; John Wiley: New York, 2000; pp 107−120.
(40) Downs, R. T.; Palmer, D. C. *Am. Mineral.* **1994**, *79* (1−2), 9−14.
(41) Spearing, D. R.; Farnan, I.; Stebbins, J. F. *Phys. Chem. Miner.* **1992**, *19(5)*, 307−321.
(42) Geisinger, K. L.; Spackman, M. A.; Gibbs, G. V. *J. Phys. Chem.* **1987**, *91*, 3237.
(43) Liebau, V. F. *Acta Crystallogr.* **1961**, *14*, 389−395.
(44) Pant, A. K.; Cruickshank, D. W. *Acta Crystallogr.* **1968**, *B24*, 13−19.
(45) Swanson, D. K.; Prewitt, C. T. *Am. Mineral.* **1983**, *68*, 581−585.
(46) Schramm, S.; Oldfield, E. *J. Am. Chem. Soc.* **1984**, *106*, 2502.
(47) Timken, H. K. C.; Janes, N.; Turner, G. L.; Lambert, S. L.; Welsh, L. B.; Oldfield, E. *J. Am. Chem. Soc.* **1986**, *108*, 7236.
(48) Clark, T. M.; Grandinetti, P. J. *Solid State NMR* **2000**, *16*, 55−62.
(49) Sternberg, U. *Solid State NMR* **1993**, *2*, 181.
(50) Newton, M. D.; Gibbs, G. V. *Phys. Chem. Miner.* **1980**, *6*, 221.
(51) Yao, Z.; Kwak, H.-T.; Sakellariou, D.; Emsley, L.; Grandinetti, P. J. *Chem. Phys. Lett.* **2000**, *327*, 85−90.
(52) Mueller, K. T.; Sun, B. Q.; Chingas, G. C.; Zwanziger, J. W.; Terao, T.; Pines, A. *J. Magn. Reson.* **1990**, *86*, 470.
(53) Vosegaard, T.; Florian, P.; Massiot, D.; Grandinetti, P. J. *J. Chem. Phys.* **2001**, *114* (10), 4618−4624.
(54) Ashbrook, S. E.; Berry, A. J.; Wimperis, S. *Am. Mineral.* **1999**, *84*, 1191−1194.
(55) Zhao, P.; Kroeker, S.; Stebbins, J. F. *J. Non-Cryst. Solids* **2000**, *276*, 122−131.
(56) Winkler, B.; Blaha, P.; Schwarz, K. *Am. Mineral.* **1996**, *81*, 545−549.